Proton Dynamics in Strong (Short) Intramolecular H-Bond. DFT Study of the KH Maleate Crystal

Mikhail V. Vener,* Alexey V. Manaev, and Vladimir G. Tsirelson

Department of Quantum Chemistry, Mendeleev University of Chemical Technology, Miusskaya Square 9, 125047 Moscow, Russia

Received: July 25, 2008; Revised Manuscript Received: October 24, 2008

The structure, harmonic frequencies, and infrared intensities of the fundamental transitions of potassium hydrogen/deuterium maleate crystals have been computed by the density functional theory with periodic boundary conditions. Different functionals with all-electron Gaussian-type orbital (GTO) basis set have been used. It was found that BLYP/GTO approximation provides the best results for the structural parameters of the KH maleate crystal. Within this approximation, the hydrogen-bonded potential in the KH maleate crystal is extremely shallow. Delocalization of the bridging protons complicates a strict definition of the space group of the crystal; the space groups *Pbcm* and $Pbc2_1$ represent an equivalent choice. The periodic BLYP/GTO study provides detailed information on the nature of the internal vibrations of the hydrogen maleate anion, which are located in the range 300−1800 cm^{-1}. Assignment of the vibrational bands in this frequency region has been performed. The two most intensive bands in the infrared spectrum (∼500 and ∼1450 cm^{-1}) are caused by the "pure" asymmetric O···H···O stretching vibrations and the stretching motion of the bridging proton heavily mixed with the C−C stretching and CH bending vibrations, respectively. A crystalline environment is found to play an important role in the low-frequency region and is negligible above 1000 cm^{-1}. The H/D substitution slightly changes the vibration frequencies, involving the stretching motion of the bridging proton because of the strong coupling between this motion and the various internal vibrations of the hydrogen maleate anion.

1. Introduction

The structure and vibrational spectra of the potassium hydrogen maleate (KHM) crystal have been investigated for more than 50 years.[1–11] The main attention was paid to the symmetry of the hydrogen maleate (H-maleate) anion and spectroscopic manifestations of the proton dynamics in strong intramolecular H-bond. Different assignments of the vibrational bands observed in the range 300−1800 cm^{-1} were proposed.[4,7,9,10] As a result, completely different forms of the strong H-bond potentials in the KHM crystal were suggested.[10–13] Ab initio computations of the structure, H-bond potential, and proton dynamics in the gas-phase H-maleate anion have been also performed.[7,14] Due to the neglect of the environmental effects, these studies have a limited applicability to the proton dynamics in molecular crystals. Wilson et al.[11] carried out plane-wave density functional theory calculations which showed a broad flat H-bond potential energy surface in KHM single crystal. However, the harmonic or anharmonic frequencies have not been evaluated in this study. Very recently, anharmonic interactions and infrared (IR) band shapes of the H-bond vibration in KHM and potassium deuterium maleate (KDM) crystals have been studied theoretically, taking into account the Fermi resonance effect and strong coupling between the H-bond vibrations and lattice phonons.[15] This paper has led to valuable insights; in particular, the general features of the IR spectrum for KHM in the region 1000−1600 cm^{-1} were described. At the same time, some important issues, e.g., the influence of crystalline environment on the structure and IR spectrum of the strong intramolecular H-bond, have still not clarified.

In the present paper, we use the periodic density functional theory (DFT) approach with all-electron Gaussian-type orbital basis set to study the structure, IR spectrum, and proton dynamics of the KHM crystal. Special attention is paid to the following problems: (i) assignment of the IR-active bands in the range 300−1800 cm^{-1} arise from the internal vibrations of the H-maleate anion; and (ii) quantitative description of the influence of crystalline environment on the frequencies and IR intensities of the fundamental transitions in the H-maleate anion.

2. Computational Methods

Two different basis sets are widely used in the periodic DFT studies of molecular crystals with H-bonds: the plane-wave (PW) and all-electron Gaussian-type orbitals (GTO). Unfortunately, IR intensities are not available for harmonic vibrations computed by DFT/PW. MD simulations should be conducted to evaluate the IR intensities using this approximation.[16,17] It is a time-consuming procedure. Moreover, the assignment of bands corresponding to stretching and bending vibrations of the bridging proton is not straightforward in some cases.[18,19] The DFT/GTO approximation was used in the present study, because the computation of the IR intensities in harmonic approximation is implemented in the CRYSTAL06 software.[20] We used the 6-31G** basis set for O, C, and H atoms because, as demonstrated earlier,[21–23] it provides reasonable results for the structure and properties of molecular crystals with H-bonds of different strengths. The basis set for K^+ ions was 8-6-5-11G.[24] The default CRYSTAL06 options were used for the level of accuracy in evaluating the Coulomb and Hartree−Fock exchange series and a grid used in evaluating the DFT exchange-correlation contribution. Tolerance on energy controlling the self-consistent field convergence for geometry optimizations and frequencies computations was set to 1×10^{-8} and 1×10^{-9}

10.1021/jp806616q CCC: $40.75
Published on Web 12/03/2008

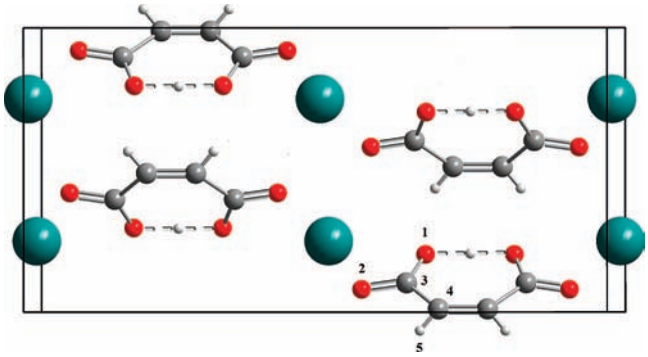

Figure 1. Molecular and crystal structure of KHM calculated by the BLYP/GTO method (the *Pbcm* space group). The red circles, large gray circles and small gray circles denote the oxygen, potassium and carbon atoms, correspondingly, while the open circles show the hydrogen atoms. Hydrogen bonds are indicated by dashed lines. The color coding of this caption also applies to Figure 4.

hartree, respectively. The number of points in the numerical first-derivative calculation of the analytic nuclear gradients equals 2. The shrinking factor of the reciprocal space net was set to 3.

3. Results and Discussion

3.1. Crystal Structure. The unit cell parameters, $a = 4.49$ Å, $b = 7.708$ Å, $c = 15.92$ Å, $\alpha = \beta = \gamma = 90.0°$, obtained in the low-temperature (5 K) neutron diffraction study[10] were adopted and structural relaxations were limited to the positional parameters of atoms. The experimental values of the atomic positions[10] were used as the starting point in the DFT/GTO computations. Three different functionals, B3LYP, BLYP, and PBE, were considered. Optimization of the internal atomic coordinates started with two different options: within the *Pbcm* space group established in the experimental study of the KHM crystal[10] and without symmetry constraints (i.e., in the space group *P*1). The structures of the *Pbcm* and *Pbc*2_1 space groups were found to correspond to the stationary points on the potential energy surface. B3LYP and PBE functionals underestimate the O···O distance in the KHM crystals on 0.03 and 0.013 Å, respectively. The BLYP/GTO approximation was found to give the best results for the structural parameters of the O···H···O fragment in the KHM crystal (Table S1). It should be noted that that the BLYP exchange-correlation functional is widely used in condensed phase computations.[25] In particular, it gives a reasonable description of the potential along the proton-transfer coordinate in the strong H-bonded crystals.[26] Therefore, the BLYP combined with the GTO approximation was used for the IR harmonic frequency computations in this work.

According to BLYP/GTO, the relative difference in the computed energies of the *Pbcm* and *Pbc*2_1 structures is about tens of wavenumbers. Both structures correspond to the minima on the potential energy surface of the KHM crystal. Variation of the CRYSTAL06 internal parameters, such as the level of accuracy in evaluating the Coulomb and exchange series, convergence criteria for the CRYSTAL06 optimizer, and the tolerance on energy controlling the self-consistent field convergence for the geometry optimization, changes the relative stability of the considered structures. However, their energies are always very close to each other: the relative difference is ± 15 cm^{-1}. The interatomic distances and valence angles computed for the KHM crystal in the *Pbcm* (Figure 1) and *Pbc*2_1 space groups are compared in Table S1 with the values obtained by the neutron diffraction of the KHM crystal at 5 K.[10]

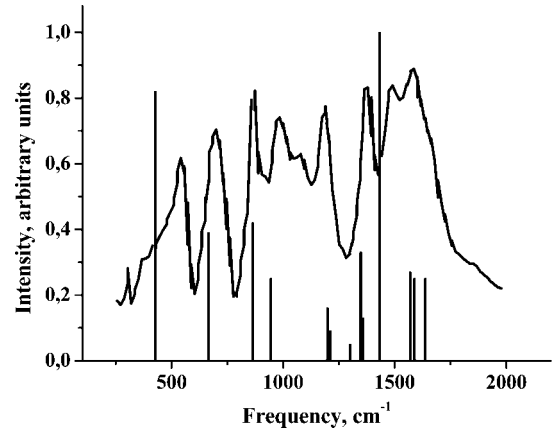

Figure 2. Observed IR spectrum of the KHM crystal in the region of the H-maleate anion internal vibrations.[9] Transition frequencies of the IR-active vibrations computed in the harmonic approximation are shown as full sticks. Their height is proportional to the relative IR intensity of the corresponding transition.

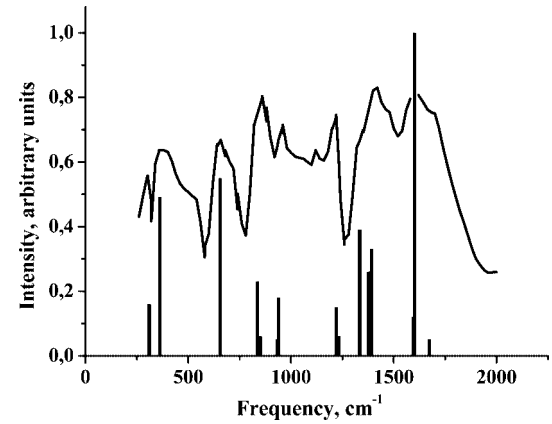

Figure 3. Observed IR spectrum of the KDM crystal in the region of the D-maleate anion internal vibrations.[9] Transition frequencies of the IR-active vibrations computed in the harmonic approximation are shown as full sticks. Their height is proportional to the relative IR intensity of the corresponding transition.

Agreement between the experimental and computed parameters can be considered as good for the O···H···O fragment and reasonable for the bond distances between the heavy atoms of the seven-member pseudocycle. The shift of the bridging proton from the midpoint between the oxygen atoms changes the space group of the crystal from *Pbcm* to *Pbc*2_1; i.e., the point symmetry group of the H-maleate anion changes from C_{2v} to C_s. Corresponding changes of the bond length (<0.001 Å) are much smaller than the typical values of the corrections of the bond distances for anisotropic thermal motion ~0.01 Å which are usually used in definition of the space group of molecular crystals with H-bonds.[27]

In summary, we found that the H-bonded potential in the KHM crystal is extremely shallow barrierless potential in accord with the results of the DFT/PW study.[11] Delocalization of the bridging protons complicates the strict definition of the space group. Centrosymmetric space group *Pbcm* and noncentrosymmetric *Pbc*2_1 structure represent an equivalent choice.

3.2. IR Spectrum. The BLYP/GTO approximation gives a reasonable description of the IR spectrum of the KHM crystal (Figure 2) and good description of the IR spectrum of the KDM crystal (Figure 3). According to our calculations, the values of the harmonic frequencies evaluated for the KHM crystal of the *Pbcm* and *Pbc*2_1 space groups are close to each other (average

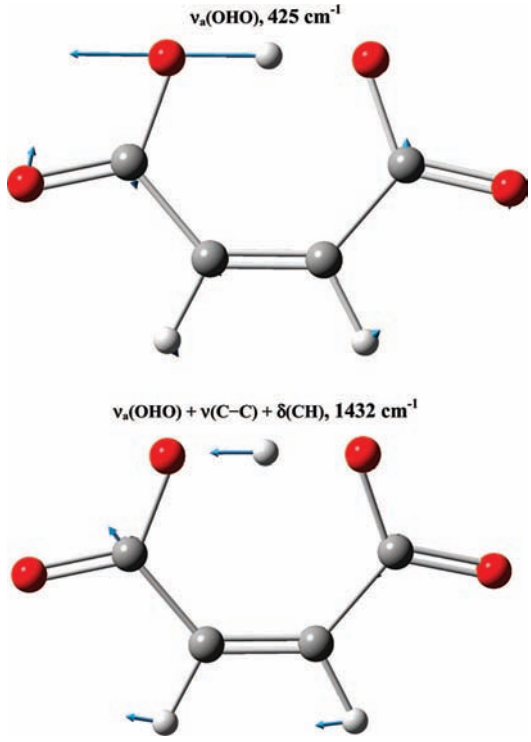

Figure 4. Schematic representation of normal coordinates for the two most intensive IR-active vibrations of the H-maleat anion in the KHM crystal. Arrows indicate directions of relative atom displacements. See the caption of Figure 1 for the color coding.

difference is a few wavenumbers). The frequencies and relative IR intensities of the fundamental transitions computed for KHM and KDM crystals within the *Pbcm* space group are compared with the experimental data in Table 1. The following conclusions can be made. (i) The computed frequencies of the carboxylate stretching and CH bending vibrations agree nicely with the experimental values. The relatively large differences around 100 cm^{-1} are obtained for the frequencies of the asymmetric stretching ν_a(OHO) and out-of-plane bending γ(OHO) vibrations. This is a consequence of the harmonic approximation. Inclusion of the anharmonicity shifts the ν_a(OHO) frequency to *blue* up to 100 cm^{-1} in very strong H-bonded systems.[28] (ii) After deuteration, IR intensities of the bands in the frequency region below 700 cm^{-1} increase considerably, in accord with a previous study.[9] (iii) The H/D substitution affects the frequencies of all vibrations, but in a different way. The isotopic ratio for frequencies of the in-plane and out-of-plane bending vibrations of the O···H···O fragment is larger than 1.3. Frequencies of the asymmetric stretching vibrations of the O···H···O fragment ν_a(OHO) shift to red, while the carboxylate stretching and CH bending vibrations shift to blue upon the deuteration. These findings are in general agreement with conclusions given in a previous study.[9]

At the same time, our study provides much more detailed information on the nature of the internal vibrations of the H-maleate anion than the traditional assignments.[4,7,9,10] Indeed, we found that a large number of vibrational bands in the range 300−1800 cm^{-1} have some partial ν_a(OHO) stretching or δ(OHO)/γ(OHO) bending character (Table 1). Special attention should be paid to the most IR-intensive band of KHM which is located around 1450 cm^{-1}. It was assigned as the "$2\nu_a$(OHO) overtone" in a previous study.[9] Computed atomic displacements for this mode are compared in Figure 4 with those of the "pure" ν_a(OHO) stretching mode with the frequency around 450 cm^{-1}. In contrast to the latter mode, in the "$2\nu_a$(OHO) overtone" mode the stretching motion of the bridging proton is heavily mixed with the C−C stretching and CH bending vibrations. This is why the most IR-intensive band of KHM is assigned as ν_a(OHO) + ν(C−C) + δ(CH), Table 1.

Summing up, explicit consideration of the crystalline environment enabled us to get a qualitatively correct description of the frequencies and relative IR intensities of the vibrations with a minor role of anharmonic effects (γ(CH), δ(CH), $\nu(CO_2)$, etc.). In the case of the vibrations involving large displacements of the bridging proton, the harmonic approximation gives a semiquantitative description of the available experimental data.

Very recently, the ab initio harmonic frequencies of the gas-phase H-maleate anion were transformed into the IR spectrum of the KHM crystal[15] using the theoretical approach[29] with the help of 9 fitting parameters. Part of the calculated bands (intense ν_a(OHO) modes at ∼1570, ∼1500, ∼1100, ∼870 and ∼540 cm^{-1}) are in good agreement with experimentally observed bands in KHM crystals.[15] This is due to appropriate account for the anharmonic effects. These effects are not considered in the present study; this is why the frequencies of the ν_a(OHO) and γ(OHO) bands differ from the experimental values (Figure 2 and Table 1). Other experimental bands of KHM were not described theoretically in ref 15 well enough, whereas they are described correctly in the present study due to the appropriate account for the crystalline-environment effects.

3.3. Influence of Crystalline Environment on the IR Spectrum. Selected frequencies computed for the gas-phase H-maleate anion and KHM crystal are compared in Table 2 with the available experimental data to reveal the influence of the crystalline environment on the IR spectrum of strong intramolecular H-bonded system. In the region below 1000 cm^{-1}, the CRYSTAL06 computations give much better results for the frequencies and IR intensities of the fundamental transitions than the gas-phase ones. In the case of the "pure" ν_a(OHO) band, the gas-phase calculations lead to the largest error (Table 2). It should be noted that the MP2/6-311++G(2d,2p) approximation gives the frequency of 170 cm^{-1} for this vibrational band; see Table 2 in ref 15. We conclude that the crystalline environment plays an important role in the case of the low-frequency vibrations involving large displacements of the bridging proton. In the frequency region above 1000 cm^{-1}, the computed values are very similar and agree with experiment. We must note that the gas-phase frequencies agree with the experimental values even better than the frequencies obtained by CRYSTAL06. On the other hand, the nature of the relative IR intensive band around 1600 cm^{-1} is different in gas phase and crystal (Table 2). In the crystal it is caused by the in-plane bending σ(OHO) vibrations while in gas phase this band resembles a strong mixing of the C═C stretching and σ(OHO) vibrations. It implies that the gas-phase data should be used with caution in simulation and/or interpretation of the IR spectra of the strongly H-bonded molecular crystals.

Table 2 shows that a frequency ratio ν_H/ν_D is close to unity for all vibrations involving the stretching motion of the bridging proton with the only exception of the "pure" ν_a(OHO) band. The ratio $\nu_H/\nu_D \sim 1$ is normally regarded as the signature of a possible double-well potential in strong *intermolecular* H-bonds;[30,31] however, this is not the case in the system under consideration. We note that the ratio $\nu_H/\nu_D \sim 1.05$ is correct for the most of the bands of the gas-phase H-maleate anion involving the stretching vibrations of the bridging proton as well; see Table 2. It implies that the low values of the ν_H/ν_D ratio are due to the *intrinsic properties* of the potential energy surface of the

TABLE 1: Comparison of the Frequencies (in cm^{-1}) and Relative IR Intensities (I/I_0) of the Fundamental Transitions Computed for KHM and KDM Crystals (*Pbcm* Space Group) in the Range 300−1800 cm^{-1} with the Experiment[9]

KHM			KDM			assignment[c]	
calcd		expt[b]			expt[b]	calcd	expt
ν (I/I_0)[a]			ν (I/I_0)				
321 (0.04)	B_{1U}	–	310 (0.16)	B_{1U}	–	δ(C═C−C)	–
406 (0.01)	B_{3U}	375 vw	405 (0.01)	B_{3U}	365 vs	δ(ring)	?
411 (0.01)	B_{2U}	410 vw	409 (0.01)	B_{2U}	410 s	δ(C═O) + δ(C═C−C)	?
425 (0.82)	B_{1U}	545 m	362 (0.49)	B_{1U}	395	ν_a(OHO)	ν_a(OHO)
–	–	618 vw	–	–	610 vw	–	$\gamma(CO_2)$
665 (0.39)	B_{1U}	690 vs	656 (0.55)	A_1	660 vs	ν_a(OHO) + $\delta(CO_2)$	ν_a(OHO)
695 (0.01)	B_{3U}	–	689 (0.01)	B_{3U}	–	δ(ring)	–
698 (0.01)	B_{2U}	–	692 (0.01)	B_{2U}	–	δ(ring)	–
836 (0.05)	B_{3U}	–	836 (0.06)	B_{3U}	–	γ(CH)	–
852 (0.04)	B_{2U}	869 vs	850 (0.06)	B_{2U}	865 vs	γ(CH)	γ(CH)
864 (0.42)	B_{1U}	895 vs	837 (0.23)	B_{1U}	895	ν_a(OHO) + δ(C═C−C)	ν_a(OHO)
944 (0.31)	B_{1U}	1000 vs	940 (0.18)	B_{1U}	960s	ν_a(OHO) + ν(C═O) + ν(C–C)	?
–	–	1075 m	–	–	1070 m	–	ν_a(OHO)
1199 (0.16)	B_{3U}	–	–	–	1192 msh	δ(CH) + γ(OHO)	δ(CH)
1211 (0.09)	B_{2U}	1205 m	1232 (0.06)	B_{2U}	1214 m		
1280 (0.03)	B_{3U}	–	921 (0.04)	B_{3U}	–	γ(OHO) + δ(CH)	–
1299 (0.05)	B_{2U}	1198 m	932 (0.05)	B_{2U}	875	γ(OHO)	γ(OHO)
1348 (0.33)	B_{1U}	1330 wsh	1334 (0.39)	B_{1U}	–	δ(CH) + ν_a(OHO)	?
1357 (0.12)	B_{2U}	1360 vs	1392 (0.33)	B_{2U}	1345 vs	$\nu(CO_2)$ + ν(C–C) + δ(CH)	$\nu_s^a(CO_2)$
1358 (0.13)	B_{3U}	1380 vs	1377 (0.26)	B_{3U}	1395 vs	$\nu(CO_2)$ + ν(C–C) + δ(OHO)	$\nu_s^s(CO_2)$
1432 (1.00)	B_{1U}	1495 vs	1390 (0.16)	B_{1U}	1420 vs	ν_a(OHO) + ν(C–C) + δ(CH)	$2\nu_a$(OHO) overtone
1569 (0.27)	B_{2U}	1580 vs	1594 (0.12)	B_{2U}	1600 vs	$\nu(CO_2)$ + δ(OHO)	$\nu_a^s(CO_2)$
1588 (0.25)	B_{3U}	1640 s	1219 (0.15)	B_{3U}	1220 s	δ(OHO)	δ(OHO)
1625 (0.02)	B_{3U}	–	1603 (0.10)	B_{3U}	–	δ(OHO) + ν(C═C)	–
1637 (0.25)	B_{1U}	1665 s	1601 (1.00)	B_{1U}	1575 vs	ν_a(OHO) + δ(C═O) + δ(CH)	ν_a(OHO)
–	–	–	1674 (0.05)	B_{3U}	1685 s	ν(C═O) + ν(C–C)	ν(C–C)
1708 (0.02)	B_{2U}	–	–	–	–	δ(OHO) + ν(C═O) + ν(C═C)	–

[a] I stands for the IR intensity of the given transition, while I_0 corresponds to the most IR-intensive vibration of the considered species; vibrations having relative IR intensities less than 0.01 are not reported. [b] Abbreviations used for relative intensities: vs, very strong; s, strong; m, medium; w, weak; vw, very weak; sh, shoulder. [c] ν, δ, and γ denote stretching, and in-plane and out-of-plane bending vibrations, respectively.

TABLE 2: Comparison of the Harmonic Frequencies (cm^{-1}), Relative IR Intensities (I/I_0), and H/D Isotopic Effect on These Frequencies, ν_H/ν_D, of the Vibrations Involving Large Displacements of the Bridging Proton Computed for the Gas-Phase H-Maleate Anion and the KHM Crystal with the Experimental Values[9]

H-maleate anion[a]			KHM crystal[b]			experiment[c]		
ν (I/I_0)[d]	μ_{eff}[e] (amu)	ν_H/ν_D	ν (I/I_0)	ν_H/ν_D	assignment	ν	ν_H/ν_D	assignment
283 (1.0)	1.7	1.25	425 (0.82)	1.17	ν_a(OHO)	549 vs	1.15	ν_a(OHO)
630 (0.18)	4.6	1.01	665 (0.39)	1.01	ν_a(OHO) + $\delta(CO_2)$	690 vs	1.09	ν_a(OHO)
862 (0.39)	4.2	1.04	864 (0.42)	1.03	ν_a(OHO) + δ(C═C−C)	895 s	∼1.0	ν_a(OHO)
919 (0.16)	2.6	1.01	944 (0.31)	1.04	ν_a(OHO) + ν(C═O) + ν(C−C)	1000 vs	1.04	?
1154 (0.06)	1.03	1.39	1299 (0.05)	1.39	γ(OHO)	1198 m	1.38	γ(OHO)
1330 (0.26)	1.5	1.02	1348 (0.33)	1.01	δ(CH) + ν_a(OHO)	1330 wsh	−	?
1386 (0.69)	3.6	1.02	1432 (1.0)	1.03	ν_a(OHO) + ν(C−C) + δ(CH)	1495 vs	1.04	$2\nu_a$(OHO) overtone
1618 (0.21)[f]	2.2	1.19	1588 (0.25)	1.30	δ(OHO)	1640 s	1.34	δ(OHO)
1674 (0.06)	6.0	1.02	1637 (0.25)	1.02	ν_a(OHO) + δ(C═O) + δ(CH)	1665 s	1.05	ν_a(OHO)

[a] The BLYP/6-31G** approximation, C_{2v} symmetry. [b] The BLYP/GTO approximation, the *Pbcm* space group. [c] Abbreviations used for relative IR intensities are introduced in Table 1. [d] I stands for the IR intensity of the given transition, while I_0 corresponds to the most IR-intensive vibration of the considered species. [e] Reduced masses of the corresponding vibrations. [f] No clearcut correlation was made between atom displacements of this normal coordinate for the gas-phase H-maleate anion and atomic displacements of the normal coordinate of the KHM crystal designated as δ(OHO).

anion. The gas-phase computations give large values of the reduced masses, from 1.5 to 7.8 amu, for the vibrations involving the stretching motion of the bridging proton (Table 2). The H/D substitution increases these values slightly, and, as a result, practically does not change the frequencies of the considered vibrations. We conclude that the ratio $\nu_H/\nu_D \sim 1$ is due to strong mixing of the ν_a(OHO) mode with the maleate skeletal vibrations. It implies that the use of the low-dimensional models for evaluating of the anharmonic frequencies (e.g., see refs 10 and 32–34) is not verified in the considered case. An adequate theoretical treatment of anharmonic frequencies and intensities in strong *intramolecular* H-bonded systems requires the use of multidimensional model Hamiltonians which treat several skeletal vibrations, e.g. the CO stretch mode, explicitly.[35,36]

We paid special attention to the theoretical description of the two very intensive bands (∼1000 and ∼1075 cm^{-1}) detected in the IR spectrum of KHM.[9] For the gas-phase H-maleate anion computations give only one IR-intensive band in this region. Its frequency is 919 cm^{-1} for BLYP (Table 2) and 967 cm^{-1} for MP2 methods; see Table 2 in ref 15. These values are close

to the frequency of the IR-active band of 944 cm^{-1} derived from CRYSTAL06 calculations (Table 2). The experimental IR-active band of 1075 cm^{-1} has no an analogue in the gas-phase or crystal computations. We can speculate that it is caused by the nonfundamental transition. In other words, this type of the structure requires a multidimensional anharmonic treatment using the accurate ab initio potential-energy and dipole-moment surfaces.[37,38]

4. Conclusions

The H-bonded potential in the KHM crystal is extremely shallow. Delocalization of the bridging protons complicates the strict definition of the space group: as a result, the noncentrosymmetric $Pbc2_1$ structure and centrosymmetric space group *Pbcm* represent an equivalent choice.

A large number of the vibrational bands of the KHM crystal in the range 300−1800 cm^{-1} have some partial ν_a(OHO) stretching or δ(OHO)/γ(OHO) bending character. The two most intensive bands in the infrared spectrum (∼500 and ∼1450 cm^{-1}) are caused by the "pure" asymmetric O···H···O stretching vibrations and the stretching motion of the bridging proton heavily mixed with the C−C stretching and CH bending vibrations, respectively.

The crystalline environment plays a crucial role in the low-frequency region and is negligible in the region above 1000 cm^{-1}. Explicit account of the crystalline-environment effects enables us to get qualitatively correct frequencies of the vibrations, with a minor role of anharmonic effects, e.g., the carboxylate stretching and CH bending modes.

Acknowledgment. This study was supported by the Russian Federal Agency for Education (Project 2.1.1.1860) and Russian Foundation for Basic Research (grant 08-03-00515-a). M.V.V. thanks Prof. Dušan Hadži, Prof. Roberto Dovesi, and Dr. Sergio Tosoni for useful comments and Drs. Alexander A. Korlyukov, Alexander Hofmann, Vadim A. Bataev, and Adam I. Stash for help in the numerical calculations.

Supporting Information Available: Interatomic distances (Å) and angles (deg) in the KHM crystal. Neutron diffraction data at 5 K (ND, 5 K) vs the BLYP/GTO values computed for the *Pbcm* and $Pbc2_1$ space groups (Table S1); tables of optimized geometries (Cartesian coordinates) for the KHM crystal computed by BLYP/GTO (the *Pbcm* and $Pbc2_1$ space groups); the output file of the calculations of vibrational frequencies with CRYSTAL06 (BLYP/GTO, the *Pbcm* space group). This information is available free of charge via the Internet at http://pubs.acs.org.

References and Notes

(1) Cardwell, H. M. E.; Dunitz, J. D.; Orgel, L. E. *J. Chem. Soc.* **1953**, 3740.
(2) Peterson, S. W.; Levy, H. A. *J. Chem. Phys.* **1958**, *29*, 946.
(3) Warlow, S. W.; Cochran, W. *Acta Crystallogr.* **1961**, *14*, 1250.
(4) Nakamoto, K.; Sarma, Y. A.; Behnke, J. T. *J. Chem. Phys.* **1965**, *42*, 1662.
(5) Maillols, J.; Bardet, L.; Marignan, R. *J. Chim. Phys.* **1969**, *66*, 539, and references therein.
(6) Tomkinson, J.; Braid, J.; Howard, J.; Waddington, T. C. *Chem. Phys.* **1982**, *64*, 151.
(7) Avbelj, F.; Hodoscek, M.; Hadzi, D. *Spectrochim. Acta A* **1985**, *41*, 89, and references therein.
(8) Zelsmann, H. R.; Mielke, Z. *Spectrochim. Acta A* **1988**, *44*, 705.
(9) Ilczyszyn, M. M.; Baran, J.; Ratajczak, H.; Barnes, A. J. *J. Mol. Struct.* **1992**, *270*, 499.
(10) Fillaux, F.; Leygue, N.; Tomkinson, J.; Cousson, A.; Paulus, W. *Chem. Phys.* **1999**, *244*, 387.
(11) Wilson, C. C.; Thomas, L. H.; Morrison, C. A. *Chem. Phys. Lett.* **2003**, *381*, 102.
(12) Fillaux, F.; Cousson, A.; Tomkinson, J. *Chem. Phys. Lett.* **2004**, *399*, 289.
(13) Wilson, C. C.; Thomas, L. H.; Morrison, C. A. *Chem. Phys. Lett.* **2004**, *399*, 292.
(14) Tian, S. X.; Li, H.-B. *J. Phys. Chem. A* **2007**, *111*, 4404, and references therein.
(15) Ratajczak, H.; Barnes, A. J.; Baran, J.; Yaremko, A. M.; Latajka, Z.; Dopieralski, P. *J. Mol. Struct.* **2008**, *887*, 9.
(16) Gaigeot, M.-P.; Sprik, M. *J. Phys. Chem. B* **2003**, *107*, 10344.
(17) Ramirez, R.; Lopez-Ciudad, T.; Kumar, P.; Marx, D. *J. Chem. Phys.* **2004**, *121*, 3973.
(18) Vener, M. V.; Sauer, J. *Phys. Chem. Chem. Phys.* **2005**, *7*, 258.
(19) Jezierska, A.; Panek, J. J.; Koll, A. *ChemPhysChem* **2008**, *9*, 839.
(20) Dovesi, R.; Saunders, V. R.; Roetti, C.; Orlando, R.; Zicovich-Wilson, C. M.; Pascale, F.; Civalleri, B.; Doll, K.; Harrison, N. M.; Bush, I. J.; D'Arco, Ph.; Llunell, M. *Crystal06 User's Manual*; Universita di Torino: Torino, Italy, 2006.
(21) Civalleri, B.; Doll, K.; Zicovich-Wilson, C. M. *J. Phys. Chem. B* **2007**, *111*, 26.
(22) Tosoni, S.; Tuma, C.; Sauer, J.; Civalleri, B.; Ugliengo, P. *J. Chem. Phys.* **2007**, *127*, 154102. 20.
(23) Vener, M. V.; Manaev, A. V.; Egorova, A. N.; Tsirelson, V. G. *J. Phys. Chem. A* **2007**, *111*, 1155.
(24) Dovesi, R.; Roetti, C.; Freyria Fava, C.; Prencipe, M.; Saunders, V. R. *Chem. Phys.* **1991**, *156*, 11.
(25) Sousa, C. F.; Fernandes, P. A.; Ramos, M. J. *J. Phys. Chem. A* **2007**, *111*, 10439.
(26) Vener, M. V. In *Hydrogen-transfer reactions. Handbook/Reference Book*; Hynes, J. T., Klinman, J. P., Limbach, H.-H., Schowen, R. L., Eds.; Wiley-VCH: Weinheim, Germany, 2006; p 273.
(27) Olovsson, I. *J. Chem. Phys.* **1968**, *49*, 1063.
(28) Vener, M. V.; Sauer, J. *Chem. Phys. Lett.* **1999**, *312*, 591.
(29) Ratajczak, H.; Yaremko, A. M. *Chem. Phys. Lett.* **1999**, *314*, 122.
(30) Hadži, D.; Orel, B.; Novak, A. *Spectrochim. Acta A* **1973**, *29*, 1745.
(31) Sokolov, N. D.; Vener, M. V.; Savel'ev, V. A. *J. Mol. Struct.* **1990**, *222*, 365.
(32) Romanowski, H.; Sobczyk, L. *Chem. Phys.* **1977**, *19*, 361.
(33) Basilevsky, M. V.; Vener, M. V. *Usp. Khim.* **2003**, *72*, 3.
(34) Kuznetsov, A. M. *Charge transfer in physics, chemistry and biology*; Gordon and Breach Science Publ.: New York, 1995.
(35) Emmeluth, C.; Suhm, M. A.; Luckhaus, D. *J. Chem. Phys.* **2003**, *118*, 2242.
(36) Matanović, I.; Došlić, N.; Kühn, O. J. *Chem. Phys.* **2007**, *127*, 014309.
(37) Vendrell, O.; Gatti, F.; Meyer, H.-D. *Angew. Chem., Int. Ed.* **2007**, *46*, 6918.
(38) Asmis, K. R.; Yang, Y.; Santambrogio, G.; Brümmer, M.; Roscioli, J. R.; McCunn, L. R.; Johnson, M. A.; Kühn, O. *Angew. Chem., Int. Ed.* **2007**, *46*, 8691.

JP806616Q